

# **Effect of Anisotropic Grain Boundary Properties on Grain Boundary Plane Distributions During Grain Growth**

Jason Gruber<sup>a</sup>, Denise C. George<sup>b</sup>, Andrew P. Kuprat<sup>b</sup>, Gregory S. Rohrer<sup>a</sup>, Anthony D. Rollett<sup>a</sup>

<sup>a</sup>Department of Materials Science and Engineering, Carnegie Mellon University, 5000 Forbes Avenue, Pittsburgh, PA 15213, USA

<sup>b</sup>Theoretical Division, Los Alamos National Laboratory, MS B221, Los Alamos, NM 87545, USA

## **Abstract**

The effects of anisotropic grain boundary properties on the evolution of boundary plane distributions were studied using three-dimensional finite element simulations of normal grain growth. The distribution of boundary planes was affected by energy anisotropy whereas no effect was observed for comparatively larger mobility anisotropy.

Keywords: Grain growth; Grain boundaries; Grain boundary energy; Grain boundary mobility; Anisotropy.

Version 12/14/04, submitted to Scripta Mater.

## **Introduction**

The distribution of grain boundary types in a polycrystalline material has been shown to affect its bulk properties, e.g. corrosion resistance [1]. Grain boundary populations are specified by the grain boundary character distribution,  $\rho(\theta, \mathbf{n})$ , which is defined as the relative areas of distinguishable grain boundaries parameterized by their lattice misorientation ( $\theta$ ) and boundary plane orientation ( $\mathbf{n}$ ). Previous experimental work has demonstrated that significant texture can appear in grain

boundary character distributions and that low energy boundaries occur in these distributions with greater frequency than higher energy boundaries [2,3].

The influence of anisotropic grain boundary properties on grain growth has been examined previously using two-dimensional grain growth simulations [4-7]. The conclusion from each of these studies was that the grain boundary energy anisotropy was more influential than mobility anisotropy in determining the distribution of grain boundary types. However, two-dimensional simulations are unable to reproduce the topological complexity of three-dimensional systems or to represent the five-dimensional domain of grain boundary character. A number of papers describe three-dimensional grain growth simulations, but these were calculated under the assumption of isotropic grain boundary properties [8-12]. One of these methods (GRAIN3D) was recently used to simulate growth in a system with anisotropic grain boundary energies and successfully reproduced an experimentally observed grain boundary character distribution [14]. The purpose of the present work is to examine the relative effects of anisotropic interfacial energy and mobility on the grain boundary character distribution in materials undergoing normal grain growth in three dimensions.

## **Simulations**

The simulation results are provided by a three-dimensional finite element model using the code GRAIN3D, which is described in detail elsewhere [12, 13]. Briefly, GRAIN3D approximates the interfaces in a grain boundary network as a mesh of triangular elements. Nodal velocities are calculated by minimizing a functional that depends on the local geometry of the mesh and the (anisotropic) properties of the grain boundaries. Grain boundary properties are assigned on the basis of the grain boundary character. The interfacial energy  $\gamma(\mathbf{g}, \mathbf{n})$  and mobility  $M(\mathbf{g}, \mathbf{n})$  functions we use are defined by an interface plane scheme, in which we imagine each boundary to

be comprised of the two surfaces bounding the grains on either side of the interface [2]. Taking  $\mathbf{n}^1$  to be the interface normal pointing into grain one and indexed in the crystal reference frame of that grain, and  $\mathbf{n}^2$  to be the interface normal pointing into grain two and indexed in the crystal reference frame of that grain, the energy and mobility are assigned in the following way:

$$E = (E(\mathbf{n}^1) + E(\mathbf{n}^2))/2 \quad (1)$$

$$M = (M(\mathbf{n}^1) + M(\mathbf{n}^2))/2 \quad (2)$$

where the functions  $E(\mathbf{n})$  and  $M(\mathbf{n})$  are chosen as

$$E = \alpha \prod_{i=1}^3 (|n_i| / \sqrt{3})^2 + 1 \quad (3)$$

$$M = \beta \prod_{i=1}^3 (|n_i| / \sqrt{3})^2 + 1 \quad (4)$$

where  $\alpha$  and  $\beta$  are positive constants. Minima for either functional then occur with normal vectors of  $\langle 111 \rangle$  type and maxima with normal vectors of  $\langle 100 \rangle$  type, as illustrated in Fig. 1. Note that Eqns. (3) and (4) imply cubic crystal symmetry. The choice of cubic symmetry minimizes the number of grain boundaries necessary to produce a statistically significant data set and simplifies the analysis. The form of the energy function is also motivated by experimental observations in Al [15].

The anisotropy of the energy function is controlled by the parameter  $\alpha$ . With  $\alpha = 0$  the function is isotropic and with  $\alpha = 0.2957$ , the ratio of the minimum to maximum energy is 1/1.25. Similarly,  $\beta$  controls the mobility anisotropy; when  $\beta = 0$  the mobility is isotropic and when  $\beta =$

13.60, the ratio of the minimum to maximum mobility is 1/12.5. Simulations were run for four situations: (1) isotropic energy and mobility, (2) isotropic energy and anisotropic mobility, (3) anisotropic energy and isotropic mobility, and (4) anisotropic energy and mobility.

The initial microstructure for each simulation was produced from a regular volume-filling tetrahedral mesh of the unit cube. Grain centers were assigned randomly to individual tetrahedra with the condition that no grain centers lie in adjacent tetrahedra. After assigning 5000 grain centers, all remaining tetrahedra were assigned to the nearest grain. To produce a relatively equiaxed structure for the simulations, isotropic grain growth was simulated in the initial microstructure until about half of the grains remained.

For each triangular element, the lattice misorientation is represented by three Euler angles  $(\alpha, \beta, \gamma)$  and the boundary orientation is represented by two spherical angles  $(\theta, \phi)$ . To characterize the relative populations of different types of boundaries, the space was partitioned into bins of equal volume with sizes of  $\Delta\alpha = \Delta\beta = \Delta\gamma = 10^\circ$  and  $\Delta\cos\theta = \Delta\cos\phi = 1/9$ . This discretization results in approximately  $6.5 \times 10^3$  physically distinct grain boundary types. Assuming an equal number of equally-sized triangle elements observed for each boundary type, for a statistically significant result it is necessary to observe at least 20 times this number of boundaries. Although each face separating two grains is represented in GRAIN3D as a number of triangular elements, the orientations of the triangles on each face are usually similar. Therefore, as a lower bound, we assume that each face contributes only one distinct orientation. The average grain is bounded by 13 to 14 facets, each of which is shared with a neighbor grain, and therefore contributes an average of about 6.5 to 7 unique boundary types. It is therefore necessary to have data from more than 20,000 grains to ensure that the total number of observations is at least 20 times the number of distinguishable boundary types. The results from 20 simulations (51,560 grains initially) have

therefore been combined to study each case. The results presented here arise from the analysis of data sets with >20,000 grains.

## Results

The grain boundary plane distributions reached a steady state after a modest amount of growth, as found previously [14]. Since the transition to a steady-state distribution is an artifact of our choice of initial microstructure, we present only those results characteristic of the steady-state behavior. Fig. 2 shows the distributions of grain boundary planes averaged over all misorientations,  $\rho(\mathbf{n})$ , after 20,000 grains (~30% of the initial value) have been eliminated. The grain boundary plane distributions for the isotropic case (Fig. 2a) and for the case with anisotropic mobility and isotropic energy (Fig. 2c) are identical and random, i.e.  $\rho(\mathbf{n})=1.0$  MRD for all  $\mathbf{n}$ . Whenever the grain boundary energy is anisotropic (Fig. 2b and Fig. 2d) the grain boundary plane distribution is also anisotropic. In the anisotropic distribution, high energy boundary planes occur less frequently than low energy boundary planes. This result is consistent both with experimental observations [2,3] and earlier simulations that did not include mobility anisotropy [14].

The grain boundary plane distributions at two fixed misorientations are shown in Fig. 3 and Fig. 4. In each case, these are the distributions after approximately 30% of the grains have been eliminated by growth. The trends observed at these misorientations are similar to those found in the misorientation averaged data (Fig. 2) and at all other fixed misorientations that were examined. When the energy is isotropic, the distribution of grain boundary planes is random, regardless of the mobility. When the grain boundary energy is anisotropic, low energy boundaries have relatively high populations and high energy boundaries occur less frequently. Note that while there is some

deviation from the exact random distribution ( $\langle \chi(\mathbf{g}, \mathbf{n}) \rangle = 1.0$  MRD for all values of  $\mathbf{g}$  and  $\mathbf{n}$ ) with anisotropic mobility, this deviation is no larger than that measured in isotropic growth.

## Discussion

The results presented here suggest that in polycrystalline materials with random orientation texture, undergoing normal, capillary driven grain growth, the distribution of grain boundary planes is determined by the anisotropy of the energy and is not influenced by the anisotropy of the mobility. This has been demonstrated by comparing data from selected points in misorientation space (Fig. 3 and 4). To show that this trend persists throughout the entire data set, all grain boundaries were grouped according to their relative energies and relative mobilities. Figure 5 shows a plot of the mean populations of all boundaries within fixed energy (or mobility) ranges for simulations with anisotropic boundary properties; the bars indicate the standard deviation of the populations. There is a clear inverse correlation between the grain boundary energy and population, as noted in an earlier experimental study [2]. By contrast, no effect of anisotropic mobility on grain boundary population was observed.

For the case examined here, the independence of the grain boundary character distribution from the mobility is noteworthy. It should be emphasized that even though the mobility anisotropy was ten times larger than the energy anisotropy, it had a negligible effect on the grain boundary character distribution. In the absence of orientation texture, it might be imagined that the highest mobility boundaries move through grains quickly and are then replaced with random boundary types, reducing the population of high mobility boundaries. However, the results in Fig. 5 demonstrate that this is not the case. In this context it is important to recognize that when the mobility is anisotropic and the energy is isotropic, then the condition for equilibrium at the triple

junctions requires that grain boundaries adopt orientations such that the grain boundary dihedral angles are all equal. Therefore, as long as the orientations of the triple lines are randomly distributed, the grain boundary plane orientations will also be randomly distributed, as is the case in Figs. 2a and 2c. On the other hand, when the boundary energy is anisotropic, the boundaries planes at triple junctions adjust to low energy orientations that also satisfy the interfacial equilibrium constraint and this produces a relatively higher population of low energy boundaries, as suggested in [6]. Finally, it should be noted that we do not necessarily expect the grain boundary character distribution to be independent of mobility when significant orientation texture is present [16].

## **Conclusion**

We have studied the relative effects of anisotropic grain boundary energy and mobility on grain boundary character distributions during normal grain growth. The assumed grain boundary energy anisotropy is shown to affect the boundary plane distribution. Boundary plane distributions exhibit relative minima (maxima) for planes at energy maxima (minima), which is consistent with experimental observations and previous simulated results. The assumed grain boundary mobility anisotropy is shown to have no measurable effect on grain boundary plane distributions.

Simulations with anisotropic energy and mobility yielded results that were similar to those obtained with anisotropic energy and isotropic mobility. These results suggest that mobility anisotropy has a relatively small effect on grain boundary plane distributions in comparison to energy anisotropy with the functions and used in this work.

## **Acknowledgement**

This work was supported by the MRSEC program of the National Science Foundation under award number DMR-0079996 and by the Computational Materials Science Network program of the Office of Basic Energy Sciences, Department of Energy.

## **References**

- [1] Randle V. *Acta Materialia* 2004;52:4067.
- [2] Saylor DM, Moraweic A, Rohrer GS. *Acta Materialia* 2003;51:3675.
- [3] Rohrer GS, Saylor DM, El-Dasher BS, Adams BL, Rollett AD, Wynblatt P. *Zeitschrift für Metallkunde* 2004;95:197.
- [4] Holm EA, Hassold GN, Miodownik MA, *Acta Materialia* 2001;49:2981.
- [5] Upmanyu U, Hassold GN, Kazaryan A, Holm EA, Wang Y, Patton B, Srolovitz DJ. *Interface Science* 2002;10:201.
- [6] Kinderlehrer D, Livshits I, Rohrer GS, Ta'asan S, Yu P. *Mat. Sci. Forum* 2004; p. 1063.
- [7] Kazaryan A, Wang Y, Dregia SA, Patton BR. *Acta Materialia*. 2002;50:2491.
- [8] Anderson MP, Grest GS, Srolovitz DJ. *Philosophical Magazine B* 1989;59:293.
- [9] Wegand D, Brechet Y, Lepinoux J, Gust W. *Philosophical Magazine B* 1999;79:703.
- [10] Wakai F, Enomoto N, Ogawa H. 2000. *Acta Materialia* 2000;48:1297.
- [11] Krill CE, Chen L-Q. *Acta Materialia* 2002;50:3057.
- [12] Kuprat AP, *SIAM Journal of Scientific Computing* 2000;22:535.
- [13] Kuprat A, George D, Straub G, Demirel MC. *Computational Materials Science* 2003;28:199.



[14] Gruber J, George DC, Kuprat AP, Rollett AD, Rohrer GS in Proceedings of the 2nd International Conference on Recrystallization and Grain Growth, B. Bacroix et al., eds. Materials Science Forum, 2004; p. 733.

[15] Saylor DM, El Dasher BS, Rollett AD, Rohrer GS. Acta Materialia. 2004;52:3649.

[16] Rollett AD. JOM 2004;56:63.

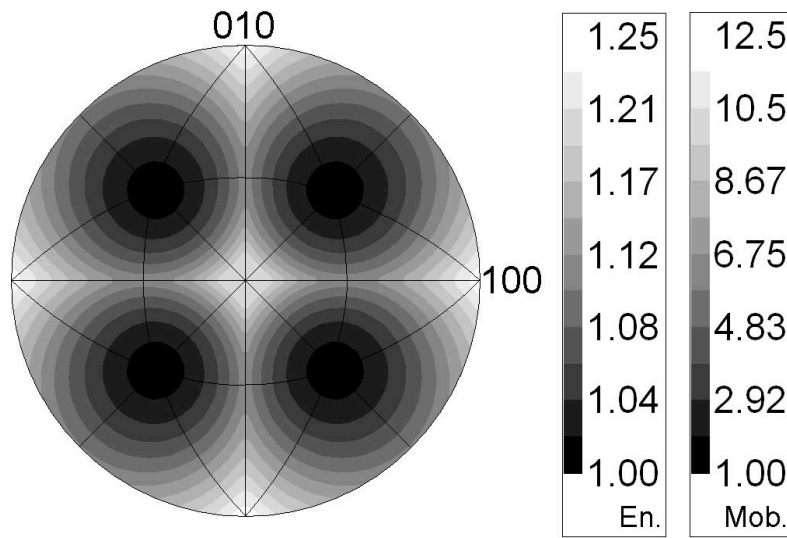


Figure 1. Energy (En.) and mobility (Mob.) as a function of interface normal vector, [001] stereographic projection. Scale values are in arbitrary units.

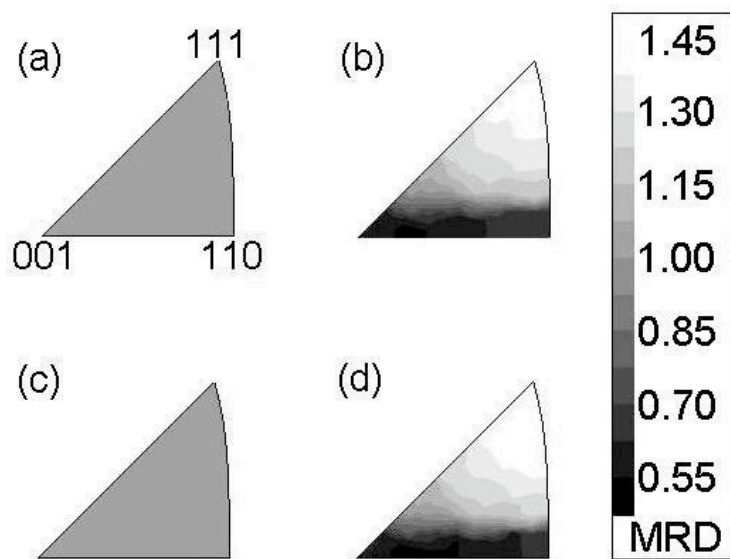


Figure 2. The distribution of boundary plane types,  $\chi(\mathbf{n})$ , independent of misorientation, for (a) isotropic growth; (b) anisotropic energy and isotropic mobility; (c) isotropic energy and anisotropic mobility; (d) anisotropic energy and mobility. Populations are measured in multiples of random distribution (MRD).

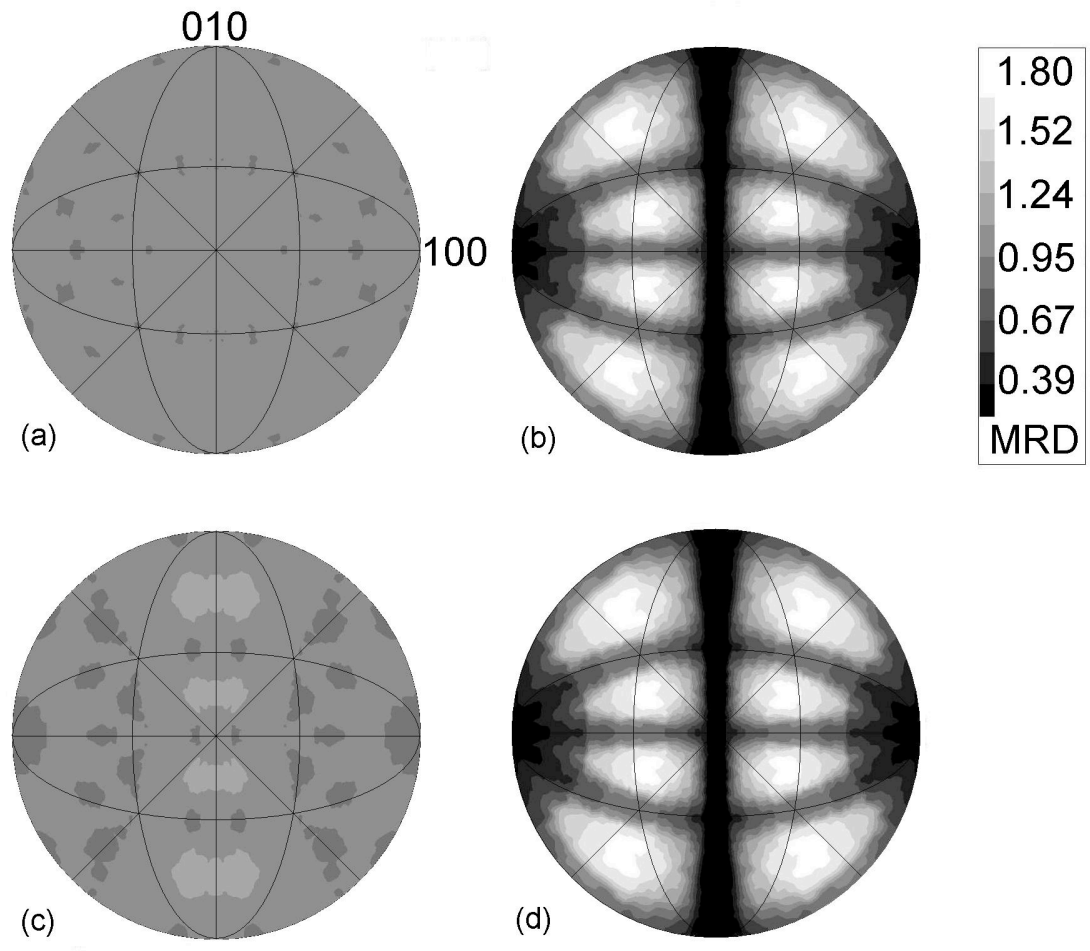


Figure 3. Grain boundary plane distributions for boundaries misoriented by  $45^\circ$  about  $[100]$ :  $\square(\mathbf{n}|45^\circ/[100])$ . (a) isotropic growth; (b) anisotropic energy and isotropic mobility; (c) isotropic energy and anisotropic mobility; (d) anisotropic energy and mobility. Populations are measured in multiples of random distribution (MRD).

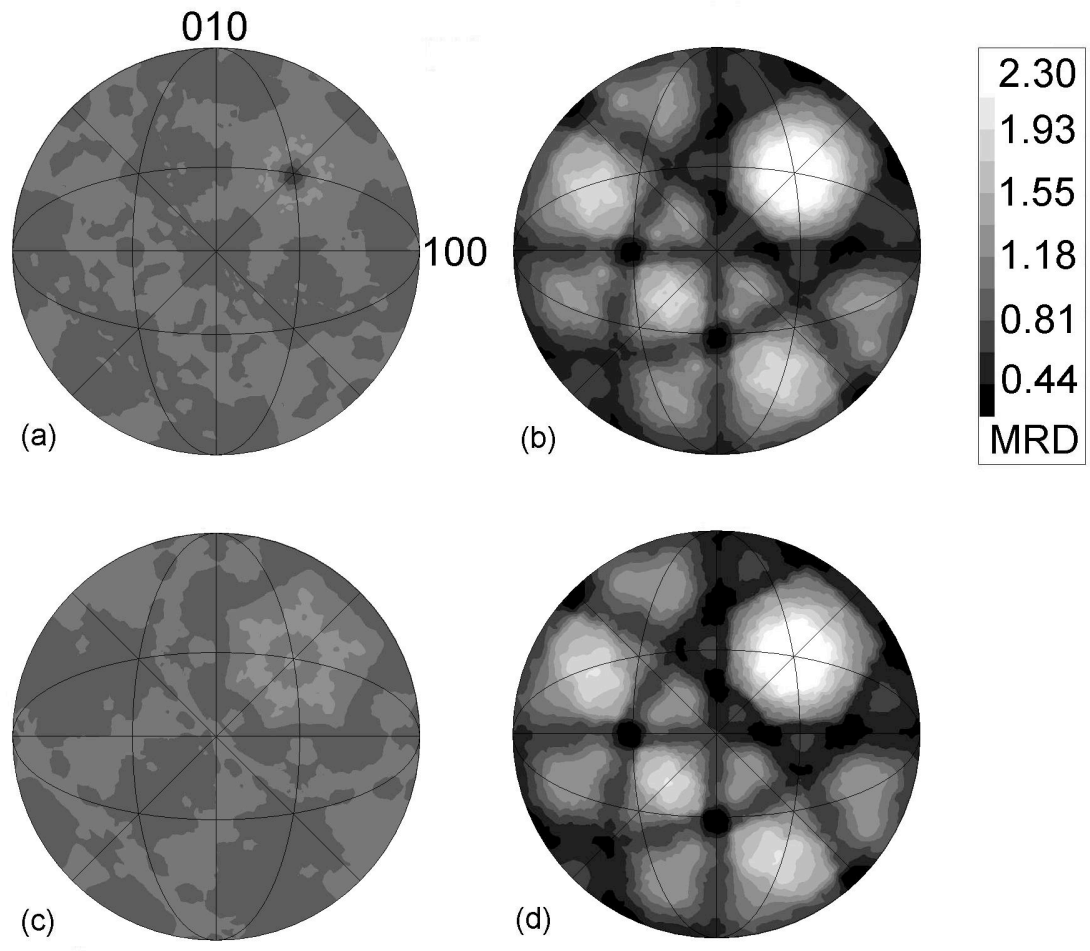


Figure 4. Grain boundary plane distributions for boundaries misoriented by  $60^\circ$  about  $[111]$ :  $\langle \mathbf{n} | 60^\circ / [111] \rangle$ . (a) isotropic growth; (b) anisotropic energy and isotropic mobility; (c) isotropic energy and anisotropic mobility; (d) anisotropic energy and mobility. Populations are measured in multiples of random distribution (MRD).

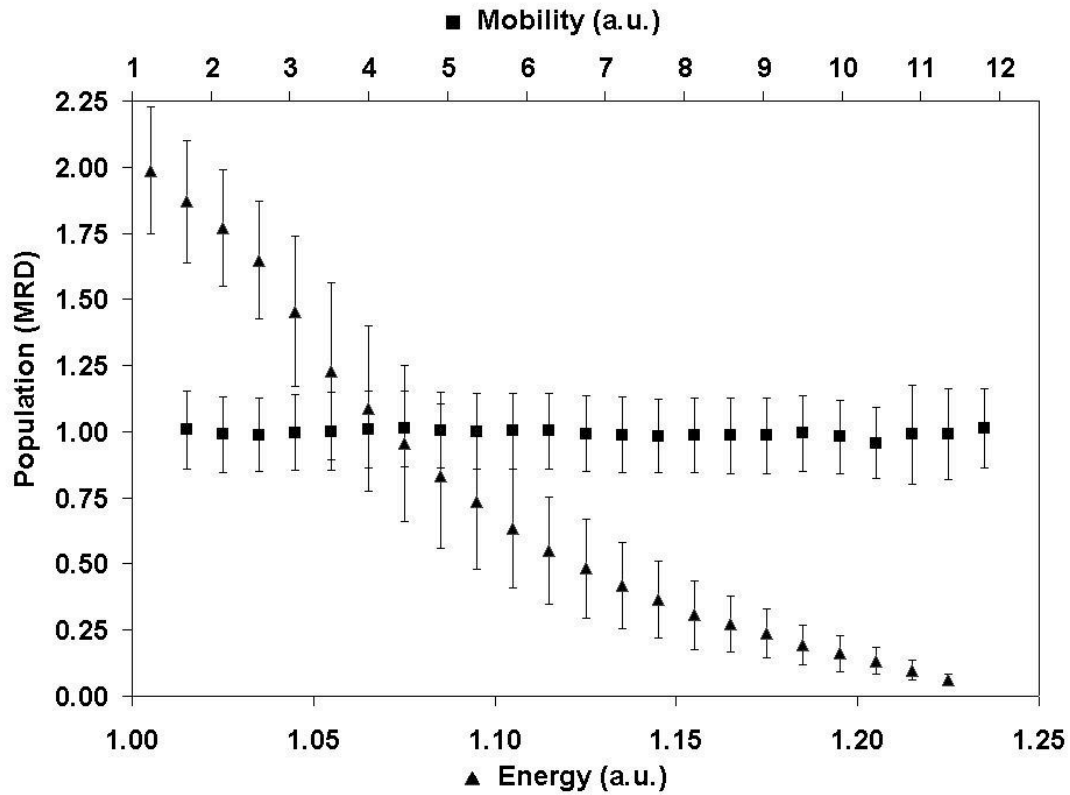


Figure 5. Average grain boundary plane population for energies within ranges of  $\pm .025$  (triangles) and mobilities within ranges of  $\pm 0.25$  (squares), over the entire domain of energy and mobility values. The energy data are from simulations with anisotropic energy and isotropic mobility. The mobility data are from simulations with anisotropic mobility and isotropic energy. Bars indicate standard deviation from local average.